

Fig. S1. TPL and TPL N176H protein interactions. (A) Semi-in vivo pull-down assays using recombinant GST N-TPL and GST N-TPL N176H fusions and transgenic *Arabidopsis* TPL-HA lysates. Immunoblotting of input shows strong transgene expression, and staining with Ponceau Red shows equal protein loading (left). Immunoblotting of control pull-down fractions (beads or GST) shows no binding, whereas both GST N-TPL and GST N-TPL N176H can bind TPL-HA (top right). Coomassie Blue staining of GST samples shows efficient expression (bottom right). (B) Model for the dominant-negative nature of *tpl-1*. The DNA-bound transcription factor AP2 represses target genes by recruiting TPL, which, like many other transcriptional co-repressors, can multimerize (left). TPL, in turn, recruits the histone deacetylase HDA19 to confer active transcriptional repression of target genes. In the absence of functional AP2, TPL-HDA19 repressor complexes are not recruited, and de-repression of target genes results (middle). Incorporation of TPL-1 mutant protein (TPL N176H) into TPL/TPR-HDA19 complexes interferes with recruitment by AP2, resulting in ectopic expression of target genes (right). This offers a plausible explanation for the dominant-negative effect of *tpl-1* on the TPL/TPR family. Consistent with this model, HDA19 has been shown to associate with at least one TPR protein (Zhu et al., 2010), although the directness of this interaction, as with HDA19-TPL binding, remains in question. The nature of TPL-protein interactions may vary between processes, as TPL N176H retains the ability to interact with repressor proteins of auxin-responsive gene expression (Szemenyei et al., 2008).

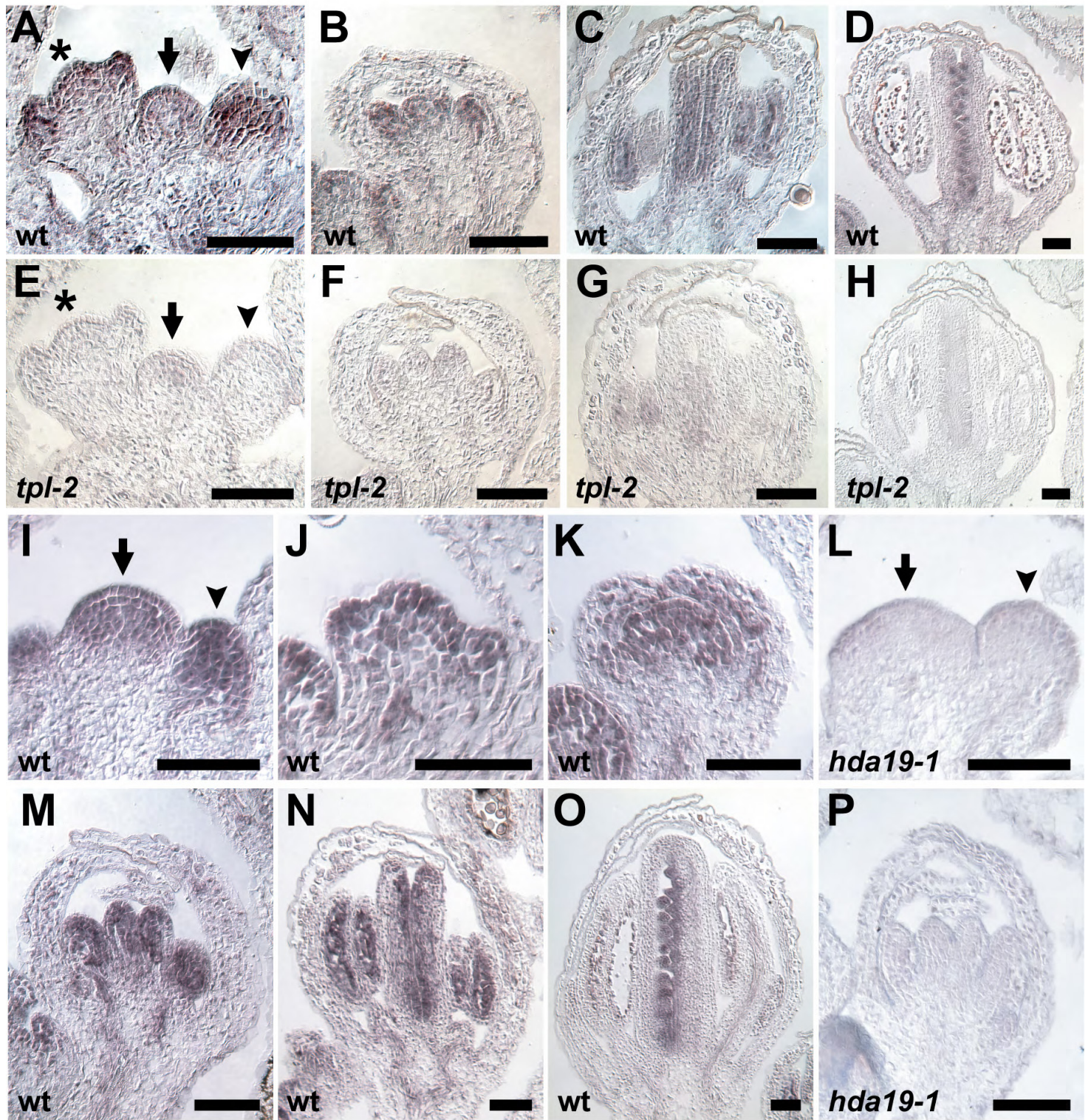


Fig. S2. Expression of *TPL* and *HDA19* in flower development. (A-H) *TPL* in situ hybridizations. (A,E) An inflorescence meristem (arrow), stage 2 floral primordium (arrowhead) and stage 3 flower (asterisk) are depicted. Note strong expression in sepal primordia at the flanks of the stage 3 flower in A. (B,F) Stage 7, (C,G) stage 9 and (D,H) stage 10 flowers. *TPL* expression is markedly reduced in *tpl-2* (E-H) relative to wild type (A-D) at all depicted floral stages. (I-P) *HDA19* in situ hybridizations. (I,L) An inflorescence meristem (arrow) and stage 2 floral primordium (arrowhead) are shown. (J) Stage 3 flower. Note expression in sepal primordia at the flanks of the floral meristem. (K) Stage 5, (M,P) stage 7, (N) stage 9 and (O) stage 10 flowers. *hda19-1* (L,P) shows vastly reduced levels of *HDA19* transcript compared with wild type at the same stages (I,M). Scale bars: 50 μ m.

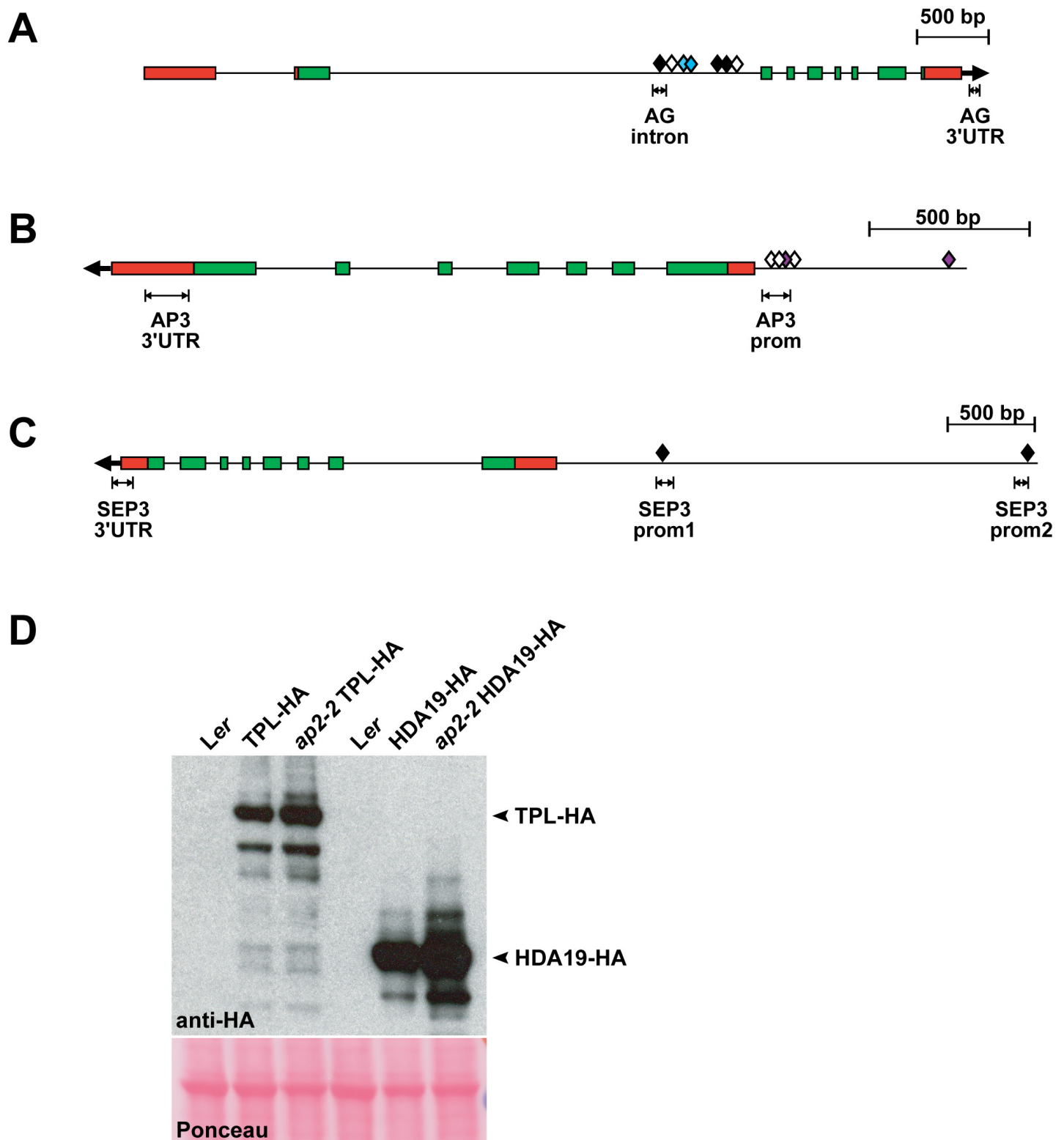


Fig. S3. ChIP PCR amplicon positions and transgene expression levels. (A-C) Positions of (A) *AG*, (B) *AP3* and (C) *SEP3* PCR amplicons used to assess enrichment in ChIP experiments shown in Fig. 2I, Fig. 3O, Fig. 5L, Fig. 6B and supplementary material **Fig. S4**. ChIP primer sequences are provided in supplementary material Table S1. Untranslated regions and exons are depicted as red and green rectangles, respectively, and black lines represent non-coding regions. Gene model arrows indicate 5'-to-3' orientation of coding sequence. Diamonds: black, AP2 binding site (Yant et al., 2010; Dinh et al., 2012); white, CArG binding sequence for MADS-domain proteins (Hill et al., 1998; Tilly et al., 1998; Kaufmann et al., 2009; Kaufmann et al., 2010b); blue, LFY/WUSCHEL paired binding sites (Busch et al., 1999; Lohmann et al., 2001); purple, LFY binding site (Lamb et al., 2002; Chae et al., 2008; Winter et al., 2011). (D) Anti-HA western blot on floral bud lysates of TPL-HA and HDA19-HA transgenic lines (used in ChIP experiments depicted in Fig. 2I, Fig. 3O and Fig. 5L). Expression of TPL-HA and HDA19-HA is at least as high in *ap2-2* as in wild type. A non-transgenic wild-type line was used as a negative control. Ponceau Red staining of blot (bottom) shows equal protein loading.

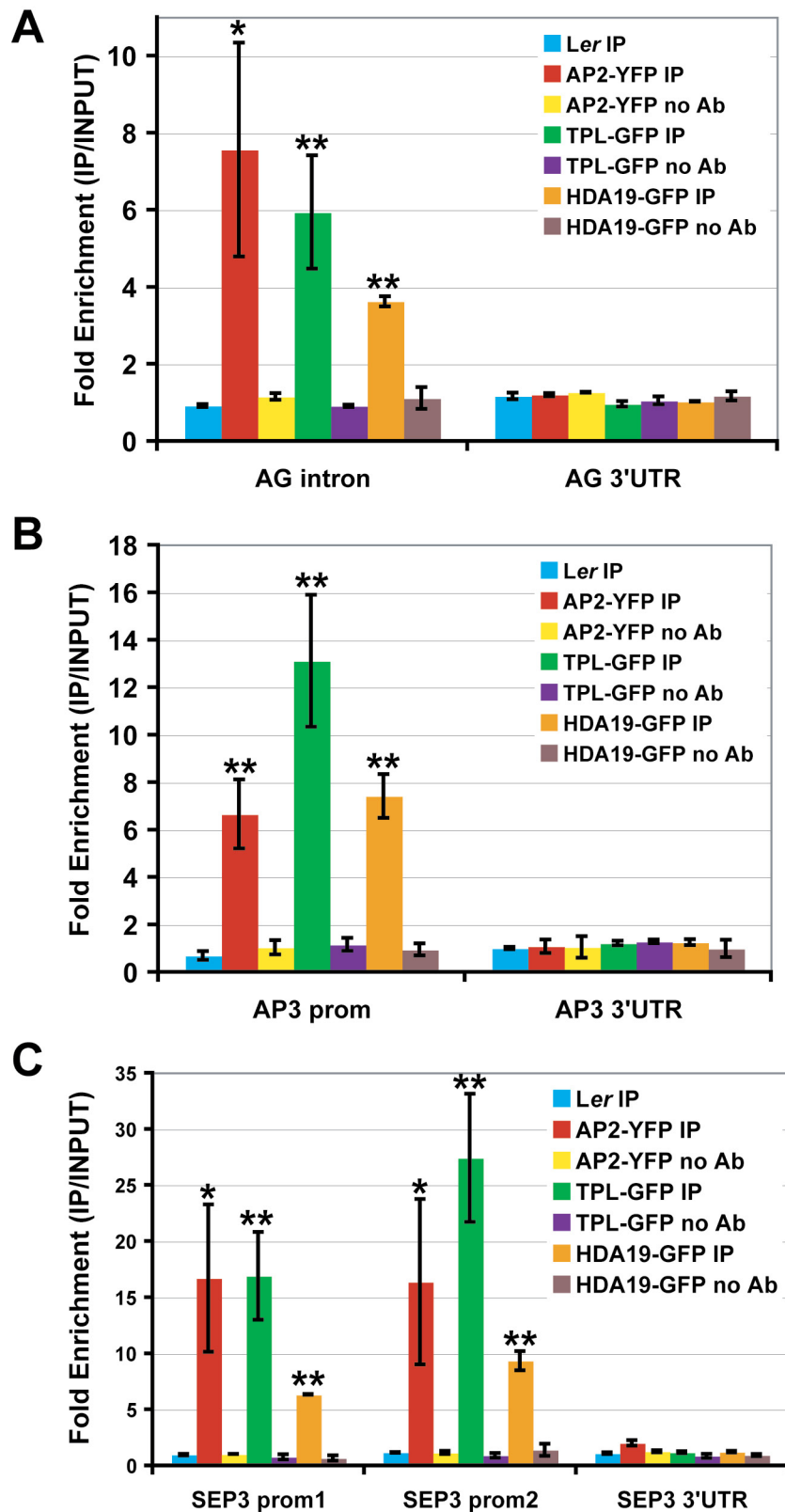


Fig. S4. Anti-GFP ChIP analyses. (A-C) Second intron of *AG* (A), promoter of *AP3* (B) and two promoter regions of *SEP3* (C) are specifically enriched in AP2, TPL and HDA19 anti-GFP ChIP samples, similar to anti-HA ChIP experiments (Fig. 2I, Fig. 3O, Fig. 5L). This enrichment is not seen in the absence of antibody (no Ab) or when using a non-transgenic wild-type (*Ler*) negative control. Positions of PCR amplicons are as in Fig. 2I, Fig. 3O, Fig. 5L and Fig. 6B and are depicted in supplementary material Fig. S3. Data were normalized relative to input and *ACT2* abundance. Data are represented as mean \pm s.e.m. of at least two biological replicates. Student's *t*-test was used to determine the significance of target enrichment relative to *Ler* IP (* $P\leq 0.1$, ** $P\leq 0.05$).

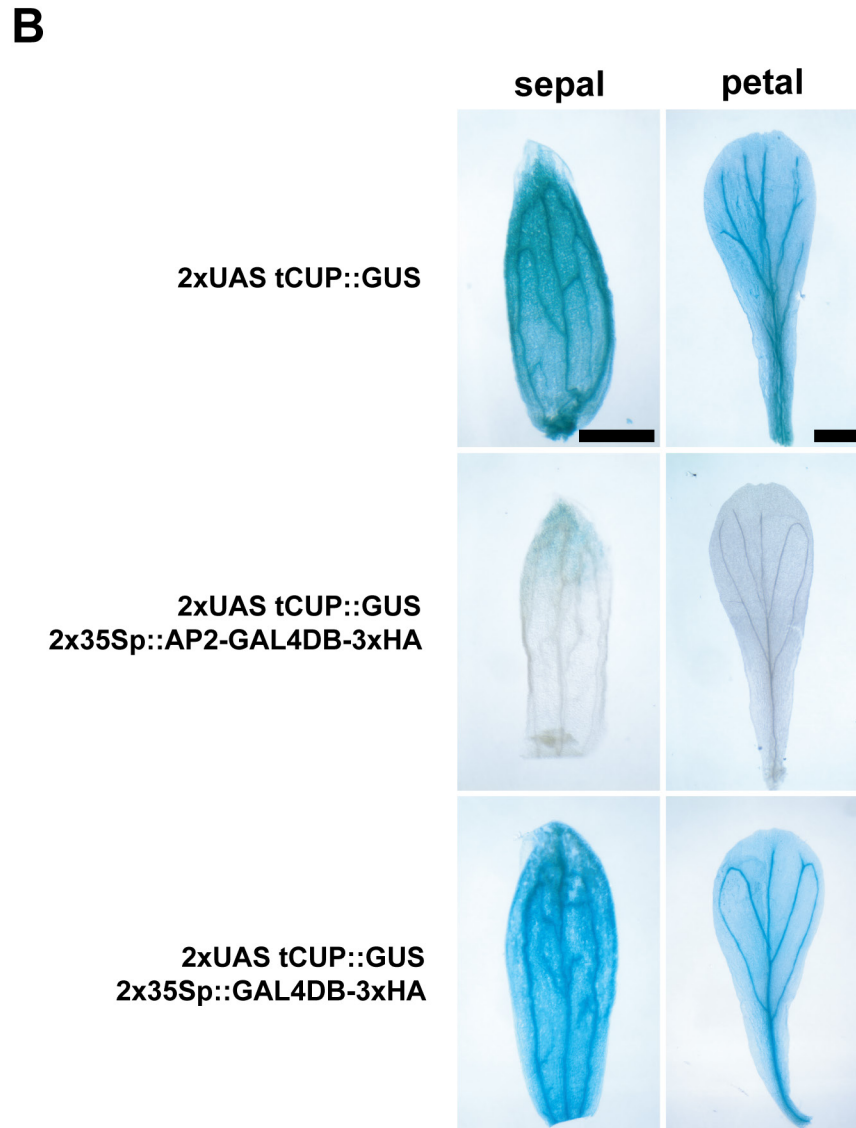
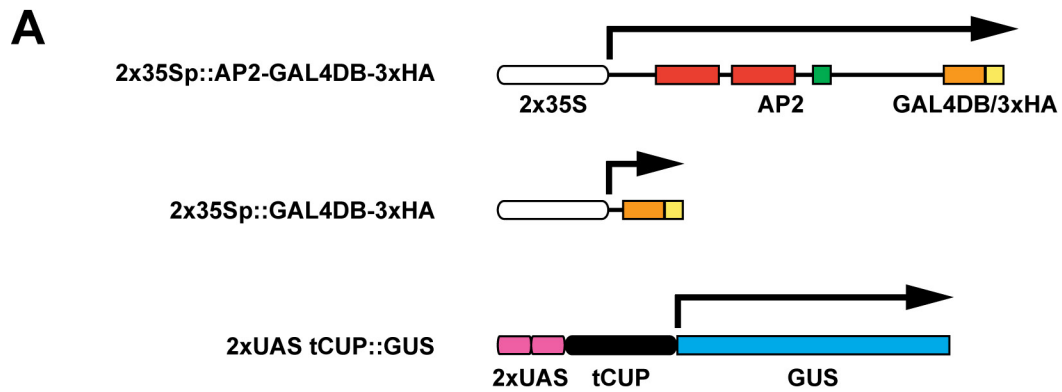


Fig. S5. AP2 transcriptional repression assay. (A) Schematics of transgenes used in repression assay. Conserved AP2 domains follow the format depicted in Fig. 1A. (B) Histochemical detection of β -glucuronidase (GUS) expression in sepals and petals. The 2xUAS tCUP::GUS reporter shows ubiquitous expression (top). Introduction of 2x35Sp::AP2-GAL4DB-3xHA strongly reduces expression of the GUS reporter in sepals and petals (middle), whereas expression of GAL4DB-3xHA alone has no effect on GUS levels (bottom).

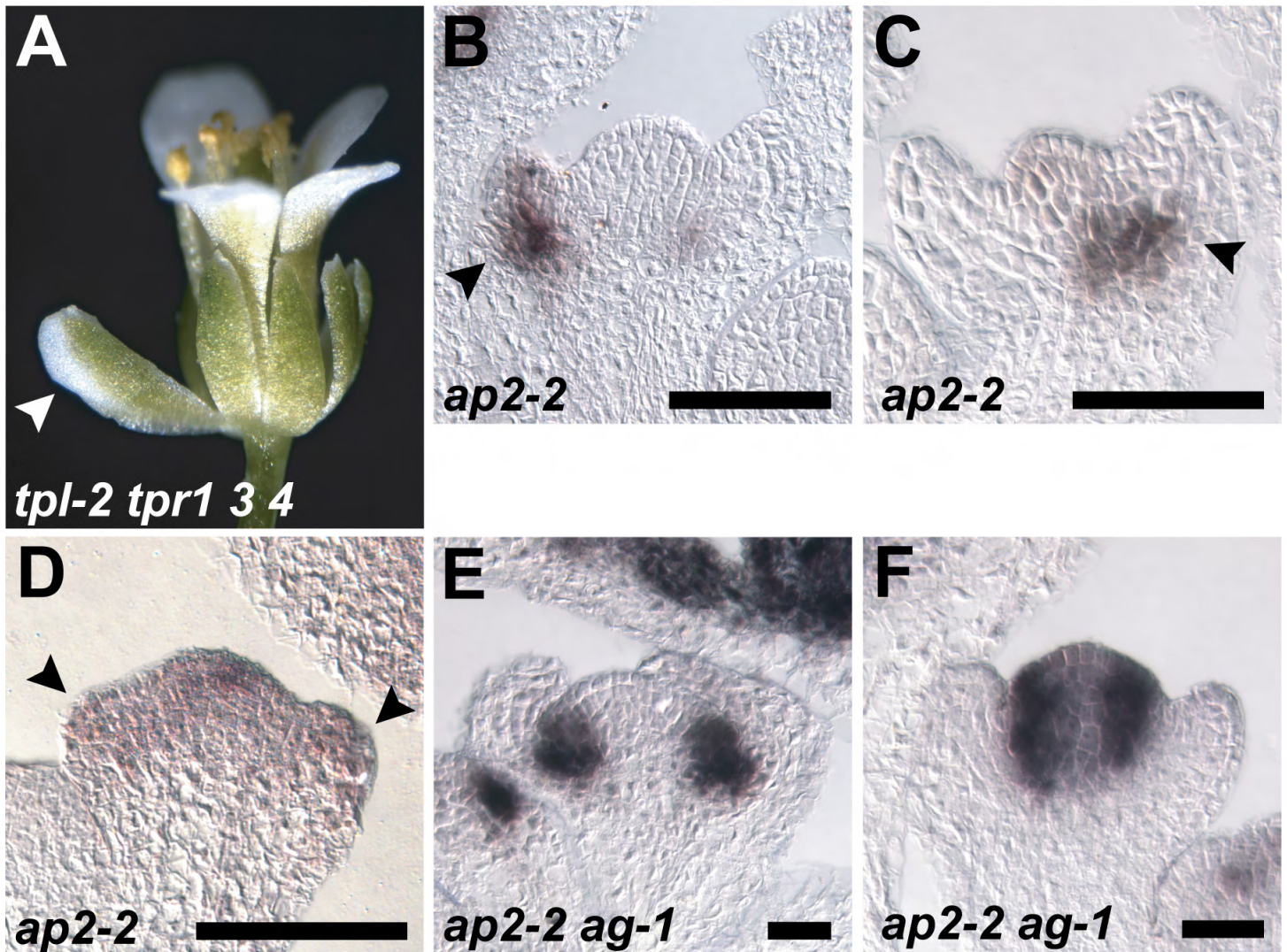


Fig. S6. Regulation of B- and E-class genes. (A) *tpl-2 tpr1 tpr3 tpr4* quadruple loss-of-function mutant flower showing sepal-to-petal conversion (arrowhead). These conversions occur less frequently in this background (<5% of whorl 1 organs) than in *tpl-1* mutants. (B,C) RNA in situ hybridizations of *ap2-2* stage 4 flowers showing ectopic *AP3* (B) and *PI* (C) expression (arrowheads). Compare with Fig. 3I and Fig. 4A, respectively. (D) *SEP3* in situ hybridization of *ap2-2* stage 3 flower displaying ectopic expression in outer whorl organ primordia (arrowheads). Compare with Fig. 5A. (E) *AP3* in situ hybridization of *ap2-2 ag-1* stage 4 flower. Compare with B and Fig. 3I. (F) *PI* in situ hybridization of *ap2-2 ag-1* stage 4 flower. Compare with C and Fig. 4A. Scale bars: 50 μm in B-D; 20 μm in E,F.

Table S1. Primers used in study.

Name	Sequence (5'-to-3')	Other
Genotyping:		
<i>tpl-1</i> F	ATGTAGTGTCCAAAGCCTTTGT	CAPS
<i>tpl-1</i> R	TTAAGCTGCGAGTTATGCAGTA	<i>AlwI</i>
<i>ap2-2</i> F	CTAGCCACCGGATCGTCCGCGGG	CAPS
<i>ap2-2</i> R	GATATCCGCTTCTACTCCACGG	<i>AlwNI</i>
<i>ag-1</i> F	GGACAATTCTAACACCGGATC	dCAPS
<i>ag-1</i> R	ATTGACCCTATCGTCTACCCATCAAAAGC	<i>HindIII</i>
<i>ap3-3</i> F	CTCTTCAACAAAAAGATTAACAAAGAGAG	dCAPS
<i>ap3-3</i> R	AACCATTCTTCTCTTTGAATACGTCAATT	<i>MfeI</i>
<i>pi-1</i> F	ATACCAGAAGTTATCTGGCAAGAAACCATG	dCAPS
<i>pi-1</i> R	GAAATTGAAAATTATTACATGATTTTGGC	<i>NcoI</i>
<i>hda19-1</i> F	GAGCTATCATCTGTTATTCAAGCCC	span
<i>hda19-1</i> R	GCAAGAAATTAGAAGCTCCGAGTC	T-DNA
<i>sep3-2</i> F	TCCTATGAGGGTCTTTGGTACACAATAATT	span
<i>sep3-2</i> R	CACTCTCTGAAGGTAGCTGAAGAAGC	transposon
Cloning:		
AP2DBs F	GACCCGGGTGCTGCTGCCGCTGCCGTAGTGGAG C	<i>SmaI</i>
AP2DBs (+miR) R	GACCCGGGGAGAATCCTGATGATGCTGCAGCG GCATTGAGTTCCTC	<i>SmaI</i>
AP2DBs (ATG) F	GACCCGGGTATGGCTGCTGCCGCTGCCGTAGTG GAGC	<i>SmaI</i>
ChIP Q-PCR:		
AG intron F	CCATCGAGAAGGTTGAGAGTTC	
AG intron R	CTTGAGTTTCCTGTATATGTA CTTG	
AG 3'UTR F	GGTACAGTTGCAAATGTCG	
AG 3'UTR R	CCGGGTGGTGAATGTATTCC	
AP3 prom F	TATCACTTAGTTTTTCATCAACTTCTG	
AP3 prom R	GAAGTAAAGGGTCCACTTGAGTTACTAA	
AP3 3'UTR F	TTTGCTGGTGCCATCATTGTCTATC	
AP3 3'UTR R	GATCACACAATCCATATTTCTTTAGGC	
SEP3 prom1 F	CATGATTCCCTGAACTCGATTTTATAAG	
SEP3 prom1 R	GGTAGGGTCTGATAAATCCACCTGATT	
SEP3 prom2 F	CAAAGCCGTCTGATTCTCATCTCAC	
SEP3 prom2 R	CTACACGACAGCTAAGTTGCGGAG	
SEP3 3'UTR F	GTTTTCTGTCTTGTGTGCATGTG	
SEP3 3'UTR R	TGGATCAGGAAGTGTAGGAGTAATGG	
ACT2 F	CTTGCACCAAGCAGCATGAA	
ACT2 R	CCGATCCAGACACTGTACTTCCTT	
H4K16Ac ChIP		
At3g18780 F	AACTGTTTAAGGTTAGATGAAGTTTG	
At3g18780 R	GCTTCTGTTCACGTACGACACTAC	
At1g59830 F	CAAAACCAAAGACGAGCCAGAGC	
At1g59830 R	ACCGAATCGTTGTAAATCGAACAC	

Table S2. Whorl 1 organ identity frequencies

	Positions scored (<i>n</i>)	% sepal	% petaloid	% petaloid/ staminoid	% staminoid	% staminoid/ carpelloid	% carpelloid	% absent	% other
<u><i>Ler</i> ecotype</u>									
Wild type	1360	100	0	0	0	0	0	0	0
<i>tpl-1</i>	1316	94.9	5.1	0	0	0	0	0	0
<i>ap2-2</i>	1252	0	0	0.1	0	18.4	66.8	12.1	2.6
<i>hda19-1</i>	1778	91.1	7.4	0	0.1	0	1.3	0	0.1
<i>tpl-1 ap2-2/+</i>	1243	48.6	39.2	3.6	5.1	0.1	1.8	1.6	0
<i>tpl-1 hda19-1</i>	1207	68.3	29.4	0.4	1.4	0.1	0.4	0	0
<i>tpl-1 hda19-1/+</i>	1192	79.8	20.1	0	0	0	0	0	0.1
<i>tpl-1 ap3-3</i>	1236	100	0	0	0	0	0	0	0
<i>tpl-1 pi-1</i>	1371	100	0	0	0	0	0	0	0
<i>hda19-1 ap3-3</i>	698	99.1	0	0	0	0	0.9	0	0
<i>hda19-1 pi-1</i>	699	99.7	0	0	0	0	0.3	0	0
<u>Col-0 ecotype</u>									
21°C:									
<i>tpl-1</i>	1872	97.3	2.4	0	0	0	0	0.3	0
<i>tpl-1 sep3-2</i>	872	99.7	0	0	0	0	0	0.3	0
29°C:									
<i>tpl-1</i>	383	91.4	6.3	1.0	0	1.0	0	0	0.3
<i>tpl-1 sep3-2</i>	562	99.8	0	0	0	0	0	0.2	0

‘Positions’ refer to individual whorl 1 floral organs, not flowers. Organs of the first 1-30 flowers produced on the primary inflorescence were scored. Floral organs resembling leaf-like structures were assigned to the ‘sepal’ category. Those described as ‘other’ included filamentous organs and rare mosaics not fitting other categories (such as petaloid/carpelloid or petaloid/staminoid/carpelloid). Although not tabulated above, the identities of whorl 1 organs at medial positions were affected to a greater extent than those at lateral positions, similar to previous reports (Bowman et al., 1991; Liu and Meyerowitz, 1995, Ng and Yanofsky, 2001).